Article

UDC 621.35:621.382.3:546.77

https://doi.org/10.31489/2025PH4/16-25

Received: 08.08.2025
Accepted: 24.10.2025

G.A. Bakalbayeva[1, 2], A.A. Baratova[1, 2]✉, N.K. Aidarbekov[1, 2], M.M. Kubenova[1, 2], A.N. Amangozhayeva[2], R.S. Bisseken[2]

[1]*Caspian University of Technology and Engineering named after Sh. Yessenov, Aktau, Kazakhstan;*
[2]*L.N. Gumilyov Eurasian National University, Astana, Kazakhstan*

Investigation of the Functional Characteristics of $Pr_{1-x}Sr_xFe_{1-\gamma}Co_\gamma O_{3-\delta}$ Perovskite Cathodes for Reversible Solid Oxide Fuel Cells

A systematic investigation was conducted on perovskite-type cathode materials of the composition $Pr_{1-x}Sr_xFe_{1-\gamma}Co_\gamma O_{3-\delta}$, synthesized via self-propagating high-temperature synthesis, with the aim of optimizing their performance in reversible solid oxide fuel cells (RSOFCs). Particular attention was given to the influence of Sr and Co substitution on thermal expansion, electrical conductivity, and polarization resistance under operating conditions. Detailed analyses using dilatometry, four-probe conductivity measurements, and electrochemical impedance spectroscopy revealed that moderate strontium substitution (x = 0.2–0.3) provides the most favorable balance between enhanced oxygen vacancy concentration, optimized lattice parameters, and structural stability. These factors jointly promote higher conductivity while maintaining low polarization resistance. The incorporation of cobalt was shown to boost electronic transport, although excessive Co levels (e.g., y = 0.5) resulted in increased thermal expansion and interfacial resistance due to phase interactions with the electrolyte. Among the studied compositions, PSFC-2020, PSFC-3020, and PSFC-4020 demonstrated superior electrochemical performance, with conductivities up to ~186 $S \cdot cm^{-1}$ and polarization resistances as low as 1.9 $\Omega \cdot cm^2$ at 850 °C. The findings confirm the potential of Pr–Sr–Fe–Co perovskites as high-performance cathode candidates for advanced RSOFCs systems, combining favorable thermomechanical compatibility, efficient charge transport, and long-term durability.

Keywords: reversible solid oxide fuel cells (RSOFCs), perovskite cathodes, Pr–Sr–Fe–Co oxides, thermal expansion, electrical conductivity, polarization resistance, electrochemical performance

✉*Corresponding author*: Baratova, Aliya, baratova_aa@enu.kz

Introduction

Reversible Solid Oxide Fuel Cells (RSOFCs), which can also operate in reverse as solid oxide fuel cells, are increasingly regarded as one of the most promising technologies for high-temperature energy conversion. These systems are not only capable of efficiently generating electricity from hydrogen and a variety of hydrocarbon fuels, but can also be employed for their electrochemical synthesis through steam electrolysis. The combination of high efficiency, flexibility in fuel choice, and significant environmental advantages positions RSOFCs as a key avenue for the advancement of hydrogen-based energy solutions [1–3].

The durability and long-term stability of such devices are largely governed by the properties of the cathode materials. These materials must combine high mixed ionic-electronic conductivity with resistance to chemical interactions and thermomechanical stresses under conditions of cyclic temperature fluctuations and varying gas atmospheres. Equally critical is their compatibility with solid electrolytes, the most widely employed of which are yttria-stabilized zirconia (YSZ) and gadolinium-doped ceria (GDC) [4–6].

Among the wide range of oxide compounds, particular attention has been drawn to complex perovskite-type materials based on rare-earth ferrite-cobaltites with the general formula $Pr_{1-x}Sr_xFe_{1-\gamma}Co_\gamma O_{3-\delta}$. Their distorted perovskite lattice with $GdFeO_3$-type orthorhombic symmetry provides a unique combination of high electrical conductivity and pronounced catalytic activity in oxygen reduction processes. The partial substitution of strontium and cobalt into the crystal structure enables deliberate tuning of oxygen non-stoichiometry, unit cell parameters, thermal expansion coefficients, and overall electrophysical properties. This flexibility offers valuable opportunities for tailoring such materials to the specific operating conditions of RSOFCs [7–9].

One of the major challenges lies in ensuring the long-term stability of cathodes under high-temperature electrolysis and repeated reversible cycling, which inherently involves alternating oxidation and reduction processes. Addressing this issue requires a comprehensive investigation of how cation composition influences the crystal structure, thermal expansion behavior, electrical conductivity, polarization resistance, and chemical compatibility of cathodes with solid electrolytes [10–12].

The present study is devoted to a comprehensive investigation of cathode materials with the composition $Pr_{1-x}Sr_xFe_{1-\gamma}Co_\gamma O_{3-\delta}$ synthesized by the self-propagating high-temperature synthesis (SHS) method. The primary objective is to identify the optimal ratios of Sr and Co that ensure maximum electrocatalytic activity, low polarization resistance, and strong resistance to degradation within high-performance RSOFCs systems. In addition, the work aims to determine the key factors governing the long-term durability and operational characteristics of these cathodes [13–15].

Materials and methods

In this work, a series of praseodymium ferrite–cobaltite perovskites with the general formula $Pr_{1-x}Sr_xFe_{1-\gamma}Co_\gamma O_{3-\delta}$ ($0 \le x \le 0.4$; y = 0.2; 0.5) was prepared using high-purity reagents to ensure accurate stoichiometry and reproducibility. The starting chemicals were praseodymium nitrate hexahydrate $Pr(NO_3)_3 \cdot 6H_2O$, iron nitrate nonahydrate $Fe(NO_3)_3 \cdot 9H_2O$, cobalt nitrate hexahydrate $Co(NO_3)_2 \cdot 6H_2O$ (purity ≥ 98–99 %), and strontium carbonate $SrCO_3$ (purity ≥ 98 %). All components were used without further purification [16–18].

The stoichiometric proportions of the precursors were calculated for each target composition, after which the reagents were dissolved in 0.1 M nitric acid (HNO_3) under continuous stirring until complete dissolution. The neutralization of $SrCO_3$ by nitric acid yielded soluble strontium nitrate with CO_2 release, while the other nitrates dissolved without secondary reactions.

The resulting homogeneous nitrate solution was evaporated to dryness, producing a mixed salt residue. This residue was dispersed in ethylene glycol ($HOCH_2CH_2OH$, ≥ 99 %) at a molar ratio of 2:1 relative to the total nitrate ion content. Ethylene glycol served simultaneously as a solvent and a fuel for the subsequent self-propagating high-temperature synthesis (SHS). Upon heating, an intense exothermic redox reaction occurred, accompanied by rapid temperature rise and the formation of finely dispersed oxide powders. Nitrogen was identified as the main gaseous by-product, indicating the high selectivity and cleanliness of the synthesis process [19–20].

The as-combusted powders underwent multi-stage heat treatment: first at 400 °C and 700 °C to remove organics and promote initial crystallization, then at 900 °C for phase development, and finally calcined at 1100 °C for 30 min to achieve complete crystallization of the perovskite structure. X-ray diffraction confirmed the high phase purity and orthorhombic $GdFeO_3$-type symmetry (*Pbnm*) for all samples.

The synthesized compositions and their corresponding abbreviations are as follows:

* PFC-20: $PrFe_{0.8}Co_{0.2}O_3$ ($x = 0$, $y = 0.2$)
* PSFC-1020: $Pr_{0.9}Sr_{0.1}Fe_{0.8}Co_{0.2}O_{3-\delta}$ ($x = 0.1$, $y = 0.2$)
* PSFC-2020: $Pr_{0.8}Sr_{0.2}Fe_{0.8}Co_{0.2}O_{3-\delta}$ ($x = 0.2$, $y = 0.2$)
* PSFC-3020: $Pr_{0.7}Sr_{0.3}Fe_{0.8}Co_{0.2}O_{3-\delta}$ ($x = 0.3$, $y = 0.2$)
* PSFC-4020: $Pr_{0.6}Sr_{0.4}Fe_{0.8}Co_{0.2}O_{3-\delta}$ ($x = 0.4$, $y = 0.2$)
* PSFC-3050: $Pr_{0.7}Sr_{0.3}Fe_{0.5}Co_{0.5}O_{3-\delta}$ ($x = 0.3$, $y = 0.5$)

In the sample code, the first two digits represent the molar fraction of Sr (x×100) and the last two digits correspond to the molar fraction of Co (y×100) in the perovskite lattice. This designation provides a clear link between composition and the measured physicochemical properties.

Table 1 presents the nomenclature and key physicochemical parameters of the synthesized $Pr_{1-x}Sr_xFe_{1-\gamma}Co_\gamma O_{3-\delta}$ perovskite powders, including specific surface area (S_{BET}), equivalent particle size (d_{BET}), and theoretical density (γ_{theo}). The series encompasses both the undoped composition (PFC-20) and Sr-, Co-substituted variants (PSFC), enabling the assessment of how A- and B-site cation substitutions influence powder characteristics.

The S_{BET} values lie in the range of 4.8–6.4 m^2/g, which is relatively high for oxide materials obtained by SHS. A gradual increase in specific surface area is observed with the introduction and growth of Sr content, as well as with partial substitution of Fe by Co. This trend may be associated with the impact of heterova-

lentcation substitution on the combustion process during SHS, where changes in thermal release and diffusion rates can limit particle coarsening and promote the formation of a more developed surface morphology.

The equivalent particle sizes (d_{BET}), calculated from BET data, range from 65 nm in PFC-20 to 50 nm in PSFC-3050, confirming the nanoscale nature of the powders. The observed reduction in particle size for Co-rich compositions can be linked to the higher exothermicity of the reaction and shortened grain growth stage, leading to enhanced dispersion. These fine particle dimensions are expected to facilitate improved contact area with the electrolyte and more efficient gas diffusion in the cathode layer.

Table 1

Nomenclature and key physicochemical parameters of $Pr_{1-x}Sr_xFe_{1-\gamma}Co_\gamma O_{3-\delta}$ perovskite powders

Sample composition	$S_{BET}(m^2/g)$	d_{BET}(nm)	γ_{theor}, g/sm^3
PFC-20	4.8	65	6.36
PSFC-1020	5.2	60	6.29
PSFC-2020	5.6	56	6.22
PSFC-3020	5.9	54	6.16
PSFC-4020	6.1	52	6.09
PSFC-3050	6.4	50	6.21

where:

– S_{BET} — specific surface area determined by the Brunauer–Emmett–Teller (BET) method;

– d_{BET}– equivalent particle diameter, calculated from S_{BET} data assuming spherical particles;

– γ_{theor} — theoretical density of the bulk perovskite phase, calculated from crystallographic parameters.

Theoretical density values (γ_{theor}) vary only slightly (6.09–6.36 g/cm^3) across the series, reflecting the fact that density is primarily determined by the crystal structure and average atomic mass of the constituent elements. Minor variations arise from the substitution of Pr^{3+} by Sr^{2+} in the A-site and Fe^{3+} by Co^{3+} in the B-site, which slightly modify the lattice parameters.

Overall, the powders synthesized via SHS demonstrate a combination of high surface area, nanoscale particle size, and phase purity, all of which are advantageous for cathode applications in RTFCs. The interplay between composition and microstructural characteristics revealed in Table 1 provides a basis for correlating synthesis conditions, structural parameters, and functional performance in subsequent electrochemical testing.

Table 2 summarizes the key ionic characteristics of the cations incorporated into the synthesized perovskites $Pr_{1-x}Sr_xFe_{1-\gamma}Co_\gamma O_{3-\delta}$, including their valence states, coordination numbers (CN), ionic radii (r), and electronegativities (χ) according to the Pauling scale. These parameters determine the strength and nature of cation–anion bonding within the crystal lattice, which in turn directly governs the coefficient of thermal expansion (CTE), electrical conductivity, and the overall electrochemical performance of the cathode materials. In particular, variations in these ionic properties critically influence lattice stability, conductivity, and the resistance of the materials under operating conditions.

A comparison of the ionic parameters of the A-site cations (Pr^{3+} and Sr^{2+}) reveals that Sr^{2+} possesses a significantly larger ionic radius (1.44 Å vs. 1.179 Å) and a lower electronegativity (0.99 vs. 1.13). Substituting Pr^{3+} with Sr^{2+} enhances the ionic character of the A–O bond and leads to an expansion of the A-site sublattice, which can contribute to an increase in the coefficient of thermal expansion by weakening the covalent component of the bonding. Moreover, the incorporation of Sr^{2+}requires charge compensation through the formation of oxygen vacancies. These vacancies not only enlarge the lattice parameters but may also strongly influence the transport properties of the material.

For the B-site cations ($Fe^{3+}$and Co^{3+}), smaller ionic radii are characteristic (0.645 Å for Fe^{3+} and 0.545–0.61 Å for Co^{3+}, depending on the spin state), along with higher electronegativity values (1.83–1.88). Incorporation of Co^{3+} not only alters the size and symmetry of the BO_6 octahedra but can also induce spin-state transitions at elevated temperatures. These transitions result in the elongation of B–O bonds and consequently contribute to an increased coefficient of thermal expansion (CTE). At the same time, such effects influence electronic and mixed ionic–electronic conductivity by modifying the orbital overlap between O 2p and B 3d states.

Table 2

Ionic parameters of cations $Pr_{1-x}Sr_xFe_{1-\gamma}Co_\gamma O_{3-\delta}$ perovskites

Sample composition	Oxidation state	Coordination Number (CN)	Ionic radius r (Å)	Electronegativity χ (Pauling)	Structural influence
Pr^{3+}	+3	9	1.179	1.13	Larger CN reduces bond distortion; higher χ leads to stronger A–O covalency
Sr^{2+}	+2	12	1.44	0.89	Lower χ increases A–O ionicity; larger radius expands lattice, affects CTE
Fe^{3+}	+3	6	0.645	1.83	Small radius stabilizes octahedral B–O bonds; higher χ strengthens covalency
Co^{3+}	+3 (low-spin/high-spin)	6	0.545 (low-spin) / 0.61 (high-spin)	1.88	Spin-state transitions at high T lengthen B–O bonds, increasing CTE

where:

– CN (Coordination Number) — the number of nearest neighboring oxygen ions bonded to a given cation within the crystal lattice;

– r(Å) — the ionic radius corresponding to the specific coordination;

– χ — the Pauling electronegativity, reflecting the ability of an ion to attract electrons.

Thus, the values presented in Table 2 provide a fundamental basis for interpreting the experimental results. They clarify why the $Pr_{1-x}Sr_xFe_{1-\gamma}Co_\gamma O_{3-\delta}$ $Pr_{1-x}Sr_xFe_{1-\gamma}Co_\gamma O_{3-\delta}$ series exhibits a nonlinear dependence of the CTE on Sr content, along with a steady increase in CTE as the Co fraction rises. Moreover, these parameters offer a physicochemical rationale for the observed trends in electrical conductivity and polarization resistance.

Results and discussion

To establish the correlation between chemical composition, structural features, thermal expansion, electrical transport behavior, and polarization resistance of the cathode materials, a series of experiments was carried out on synthesized perovskites $Pr_{1-x}Sr_xFe_{1-\gamma}Co_\gamma O_{3-\delta}$ with controlled Sr and Co contents.

The linear CTE was measured using a Netzsch DIL 402C dilatometer over the temperature range from room temperature up to 1000 °C at a heating rate of 5 °C/min. The influence of Sr and Co on the CTE can be explained by their ionic characteristics (Table 2):

– substitution of Pr^{3+} (χ = 1.13, r = 1.179 Å, CN = 9) with Sr^{2+} (χ = 0.99, r = 1.44 Å, CN = 12) enlarges the A-site sublattice and modifies the strength of the A–O bond, which can either increase or decrease the CTE.

– the incorporation of Sr^{2+} requires charge compensation through the formation of oxygen vacancies, which expand the lattice and promote higher CTE values.

– doping with Co^{3+} (particularly in its high-spin state) leads to elongation of the B–O bonds at elevated temperatures due to spin-state transitions, thereby producing a consistent increase in the CTE.

Electrical conductivity was measured on rectangular bars (3×2×30 mm) prepared by uniaxial pressing followed by sintering at 1100 °C for 4 h. Platinum electrodes (0.2 mm) were applied with platinum paste and subsequently fired at 900 °C for 1 h. Measurements were carried out in air using a four-probe DC technique (Solartron SI-1260/1287) over the temperature range of 300–950 °C with 50 °C increments. Increasing the Sr content up to $x = 0.2$ reduced the activation energy (E_a) and enhanced the conductivity due to a higher carrier concentration and reduced lattice distortions. At higher Sr levels ($x \geq 0.3$), the conductivity effect tended to stabilize, indicating saturation of the defect structure.

Polarization resistance (Rη) was determined by electrochemical impedance spectroscopy (EIS) using symmetric cells with dense YSZ and GDC electrolytes. Electrolyte discs (~12 mm in diameter, 0.3 mm thick) were pressed at 300 MPa and sintered at 1450 °C (YSZ) or 1350 °C (GDC). Cathode layers with a thickness of 20–30 μm were deposited by screen printing from a slurry composed of perovskite powder, iso-

propanol, polyvinyl butyral, and triethylene glycol dimethacrylate. The firing process was carried out at 1050 °C (for PSFC-3020) to optimize adhesion to the electrolyte and minimize the formation of secondary phases.

Impedance measurements were conducted in the frequency range of 0.1 Hz to 1 MHz with an amplitude of 10 mV in air at 600–900 °C, using 50 °C increments. By combining thermomechanical, electrical transport, and electrochemical characterization with an analysis of the cationic ionic parameters, it was possible to establish a balance between structural stability, high electrical conductivity, and low polarization resistance. Among the investigated compositions, PSFC-2020, PSFC-3020, and PSFC-4020 demonstrated the most promising performance as cathode materials for RSOFCs when paired with YSZ and GDC electrolytes.

Figure 1 illustrates the variation of the linear thermal expansion coefficient (CTE, α) in the low-temperature region for the $Pr_{1-x}Sr_xFe_{1-\gamma}Co_\gamma O_{3-\delta}$ (PSFC-x20) series with different molar fractions of Sr (x = 0–0.4), as well as for the specific composition $Pr_{0.7}Sr_{0.3}Fe_{0.5}Co_{0.5}O_{3-\delta}$ (PSFC-3050).

The PSFC-x20 curve exhibits a distinctly nonlinear behavior. In the range $0 < x \leq 0.1$, a slight increase in α is observed, followed by a decrease at x = 0.2 and 0.3. The lowest CTE values are recorded at x = 0.3, indicating an optimal balance between lattice parameters and defect concentration in this compositional region. With further Sr substitution up to x = 0.4, a sharp rise in α occurs.

This behavior can be explained by the competition of two mechanisms:

– the enhancement of the ionic character of the A–O bond when Pr^{3+} (χ = 1.13) is substituted with the less electronegative Sr^{2+} (χ = 0.99) increases lattice rigidity and reduces its tendency toward thermal expansion.

– at the same time, the growth in oxygen vacancy concentration, required for charge compensation upon Sr^{2+} incorporation, weakens interstitial bonding and promotes higher CTE values.

For compositions with $x \leq 0.3$, the first mechanism dominates, resulting in a reduction of α, whereas for $x > 0.3$ the second mechanism prevails, leading to an increase.

The specific composition PSFC-3050, which contains a higher Co fraction (y = 0.5), exhibits a markedly higher CTE compared with PSFC-3020 at the same Sr content (x = 0.3). This behavior is consistent with the well-documented effect of spin-state transitions of Co^{3+} upon heating, which are accompanied by the elongation of Co–O bonds and, consequently, an increase in thermal expansion.

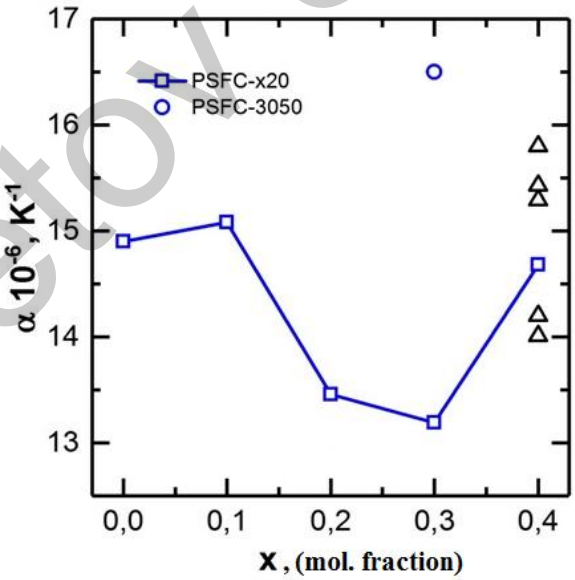

Figure 1. Dependence of the linear thermal expansion coefficient (α) of $Pr_{1-x}Sr_xFe_{1-\gamma}Co_\gamma O_{3-\delta}$ and $Pr_{0.7}Sr_{0.3}Fe_{0.5}Co_{0.5}O_{3-\delta}$ compositions on Sr molar fraction (x) in the low-temperature range

From the standpoint of minimizing the CTE and achieving better thermomechanical compatibility with solid electrolytes (YSZ and GDC), the most promising compositions are those with moderate Sr content (x = 0.2–0.3) and reduced Co content, particularly PSFC-2020 and PSFC-3020.

Figure 2 presents the temperature dependence of the electrical conductivity (σ) for a series of perovskite compositions with varying Sr and Co contents in the range of 350–950 °C.

For the PFC-20 composition ($x = 0$, $y = 0.2$), which does not contain Sr, an exponential increase in conductivity with temperature was recorded, showing no indication of saturation-behavior typical of thermally activated charge transport. A similar trend is observed for PSFC-1020 ($x = 0.1$, $y = 0.2$), though at a noticeably higher conductivity level. This enhancement is attributed to the effect of Sr^{2+}, which promotes the formation of oxygen vacancies and increases the concentration of mobile charge carriers.

Compositions with higher Sr contents ($x = 0.2$–0.4) exhibit nontrivial temperature-dependent behavior: in the conductivity curves of PSFC-2020, PSFC-3020, PSFC-4020, and particularly PSFC-3050, a distinct maximum is observed, followed by a decline at elevated temperatures. Such behavior is characteristic of mixed-conducting oxides, where increasing temperature enhances oxygen release. The resulting oxygen loss reduces the concentration of hole carriers (e.g., Fe^{4+}), thereby disturbing the balance between ionic and electronic conductivity.

The temperatures corresponding to the conductivity maxima (T_{max}) systematically shift toward lower values with increasing Sr content. This trend reflects the role of oxide non-stoichiometry: higher Sr^{2+} concentrations accelerate the generation of oxygen vacancies, lowering the lattice stability against thermal degradation. At the same time, varying the Co fraction for instance, in PSFC-3050 with y = 0.5 leads to a significant increase in the absolute conductivity values, while exerting only a minor effect on the position of T_{max}.

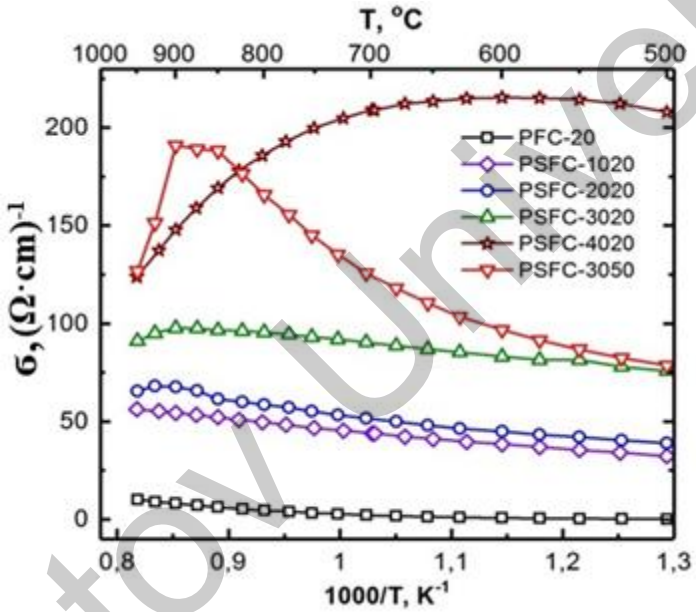

Figure 2. Dependence of the linear thermal expansion coefficient (α)
of temperature-dependent electrical conductivity of $Pr_{1-x}Sr_xFe_{1-\gamma}Co_\gamma O_{3-\delta}$

The coincidence of T_{max} with the inflection points in the CTE curves—as demonstrated earlier—highlights the close relationship between the electrophysical and structural properties of the investigated materials. Among the studied compositions, PSFC-2020 and PSFC-3020 exhibit the most stable conductivity within the operating temperature range, maintaining a balance between sufficient mobile carrier concentration and resistance to oxygen-related degradation. These materials are therefore particularly promising for cathode applications in RSOFCs operating under high-temperature conditions.

Of particular interest is the PSFC-3050 composition, which exhibits an anomalous temperature dependence of conductivity. This behavior necessitated the calculation of two distinct activation energy values: 16.0 kJ·mol^{-1} in the 300–600 °C range and 30.5 kJ·mol^{-1} in the 600–850 °C range. Such a distinction suggests a change in the dominant charge-transport mechanisms across different temperature intervals.

The polarization resistance values also clearly highlight the advantage of Sr-rich compositions. The lowest Rη values (1.9–2.5 Ω·cm^2) were recorded for PSFC-2020, PSFC-3020, and PSFC-4020, indicating high-quality cathode/electrolyte interfaces and reduced losses associated with electrode reactions.

Thus, the most promising candidates for application as dense cathodes in RSOFCs are PSFC-4020 and PSFC-3050, which combine high electrical conductivity, reduced polarization resistance, and acceptable thermal stability.

Figure 3 illustrates the dependence of the polarization resistance (Rη) of the PSFC-3020 cathode material on the sintering temperature applied to bond it with the YSZ solid electrolyte, measured at an operating temperature of 850 °C. The results clearly show that the polarization resistance reaches its minimum when sintering is carried out at 1050 °C.

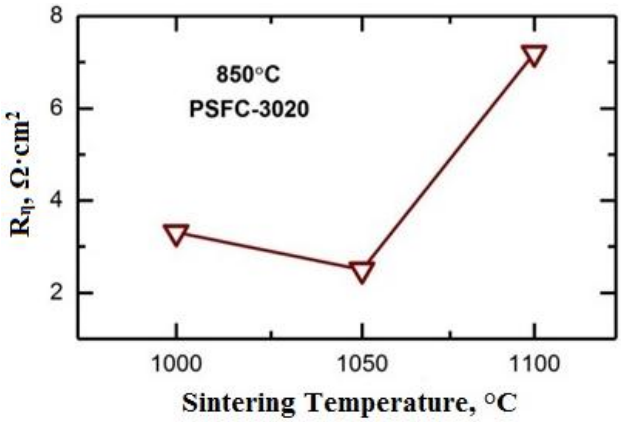

Figure 3. Influence of the sintering temperature on the polarization resistance of the PSFC-3020 cathode in contact with a YSZ electrolyte

Figure 4 presents the dependencies of electrical conductivity (σ) and polarization resistance (Rη) for cathode materials of the composition $Pr_{1-x}Sr_xFe_{0.8}Co_{0.2}O_{3-\delta}$ as a function of the Sr molar fraction (x) at 850 °C.

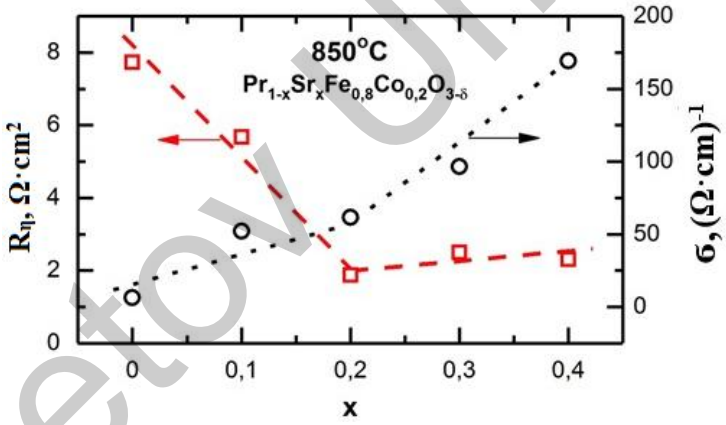

Figure 4. Effect of Sr Content on the Electrical Conductivity and Polarization Resistance of $Pr_{1-x}Sr_xFe_{0.8}Co_{0.2}O_{3-\delta}$ Cathodes at 850 °C

Up to x = 0.2, a clear correlation is observed between the two parameters: as electrical conductivity increases, polarization resistance decreases significantly. This relationship indicates improved kinetics of oxygen electrochemical processes, driven by a higher density of charge carriers and enhanced interfacial charge transfer.

However, for x > 0.2, the trend changes: despite the continued rise in electrical conductivity, polarization resistance begins to increase. This discrepancy is most likely associated with chemical interactions between Sr-enriched cathodes and the YSZ electrolyte during thermal treatment, leading to the formation of low-conductivity secondary phases at the electrode/electrolyte interface. This effect is particularly pronounced in the PSFC-3050 sample, which exhibits high Rη despite its relatively high σ, supporting the above interpretation.

Therefore, the optimal balance between high electrical conductivity and low polarization resistance is achieved at Sr concentrations in the range of 0.2–0.3 molar fraction. Within this composition window, PSFC-2020, PSFC-3020, and PSFC-4020 show the most favorable electrochemical performance among the studied materials.

Conclusion

This work presents an in-depth study of the structural, electrical, and electrochemical characteristics of perovskite-type cathode materials based on $Pr_{1-x}Sr_xFe_{0.8}Co_{0.2}O_{3-\delta}$, synthesized via a self-propagating high-temperature synthesis route. By systematically varying the Sr and Co content, a series of compositions was prepared and thoroughly evaluated in terms of thermal expansion behavior, electrical conductivity, and polarization resistance under conditions relevant to reversible solid oxide fuel cells (RSOFCs).

It was shown that moderate strontium substitution (x = 0.2–0.3) leads to improved electrochemical performance due to enhanced oxygen vacancy concentration and optimized lattice parameters, which facilitate effective charge transport. The incorporation of cobalt further promotes electronic conductivity and structural flexibility, though excessive Co levels (e.g., in PSFC-3050) were found to negatively impact polarization resistance, likely due to undesirable interfacial phase formation with the YSZ electrolyte.

Among the studied compositions, PSFC-2020, PSFC-3020, and PSFC-4020 demonstrated a balanced combination of high electrical conductivity (up to ~186 $S \cdot cm^{-1}$ at 800 °C) and low polarization resistance (as low as 1.9 $\Omega \cdot cm^2$ at 850 °C), along with favorable thermal compatibility with common electrolytes. Notably, PSFC-3020 exhibited optimal performance at a sintering temperature of 1050 °C, minimizing interfacial degradation and ensuring good adhesion to the YSZ substrate.

These findings confirm that tailored A-site (Sr) and B-site (Co) substitution within the Pr-based perovskite structure enables precise control over the functional properties of cathode materials. The study highlights the potential of PSFC-type materials as high-performance cathodes for advanced RSOFCs systems, offering improved energy efficiency, electrochemical stability, and long-term durability.

Acknowledgment

This research has been funded by the Science Committee of the Ministry of Science and Higher Education of the Republic of Kazakhstan (Grant No. BR24992964).

References

1 Minh, N. & Williams, M. C. (2015). Electrolysis operating mode for reversible solid oxide fuel cells. *ECS Transactions, 68*(1), 3301–3305. https://doi.org/10.1149/06801.3301ecst

2 Yoon, K.J., Lee, S., Park, S.-Y., & Minh, N.Q. (2025). Advances in high-temperature solid oxide electrolysis technology for clean hydrogen and chemical production: Materials, cells, stacks, systems and economics. *Progress in Materials Science, 154*, 101520. https://doi.org/10.1016/j.pmatsci.2025.101520

3 Liang, Z., Wang, J., Ren, K., & Jiao, Z. (2024). Discovering two general characteristic times of transient responses in solid oxide cells. *Nature Communications, 15*(1), 4587. https://doi.org/10.1038/s41467-024-48785-1

4 Yerofeev, V., Goncharova, M., Smirnov, V., Rodin, A., & Volkov, A. (2025). Bio-resistant cement composites with active mineral additive. *International Journal for Computational Civil and Structural Engineering, 21*(3), 33–40. https://doi.org/10.22337/2587-9618-2025-21-3-33-40

5 Güneş, F. & Korkmaz, T. (2025). Comparison of the mechanical properties of polyetheretherketone and polyphenylenesulfone produced by fused filament fabrication and conventional manufacturing methods for dental applications: An in vitro study. *BMC Oral Health, 25*, 1455. https://doi.org/10.1186/s12903-025-06851-0

6 Zhang, Z., Wang, X., & Yan, Y. (2021). A review of the state-of-the-art in electronic cooling. *e-Prime Advances in Electrical Engineering, Electronics and Energy, 1*, 100009. https://doi.org/10.1016/j.prime.2021.100009

7 Zheng, H., Li, W., Ma, S., Li, Z., Chen, Z., Zhang, L., Hu, J., & Liu, T. (2025). Perovskite oxides for electrocatalytic nitrogen/carbon fixation. *Chemical Science.* Advance Article. https://doi.org/10.1039/D5SC05965H

8 Assirey, E.A. (2019). Perovskite synthesis, properties and their related biochemical and industrial application. *Saudi Pharmaceutical Journal, 27*(6), 817–829. https://doi.org/10.1016/j.jsps.2019.05.003

9 Wang, J., Chao, G., Zong, W., Chu, K., Zhu, J., Chen, R., Zheng, Y., Zhang, L., & Liu, T. (2024). Efficient nitrate electroreduction to ammonia over copper catalysts supported on electron-delocalized covalent organic frameworks. *Chemical Engineering Journal, 499*, 156343.https://doi.org/10.1016/j.cej.2024.156343

10 Mirza, M., Abdulaziz, R., Maskell, W. C., Wilcock, S., Jones, A. H., Woodall, S., Jackson, A., Shearing, P.R., & Brett, D.J.L. (2023). Electrochemical processing in molten salts — a nuclear perspective. *Energy & Environmental Science, 16*, 952–982. https://doi.org/10.1039/D2EE02010F

11 Zong, S., Zhao, X., Jewell, L.L., Zhang, Y., & Liu, X. (2024). Advances and challenges with SOEC high temperature co-electrolysis of CO_2/H_2O: Materials development and technological design. *Carbon Capture Science & Technology, 12*, 100234. https://doi.org/10.1016/j.ccst.2024.100234

12 Franco, A. (2025). Green hydrogen and the energy transition: Hopes, challenges, and realistic opportunities. *Hydrogen, 6*(2), 28. https://doi.org/10.3390/hydrogen6020028

13 Nikolaev, K.G., Wu, J., Leng, X., Vazquez, R.J., McCuskey, S.R., Bazan, G.C., Novoselov, K.S., & Andreeva, D.V. (2025). A single-material strategy: Graphene sponge bioanode and cathode for Shewanellaoneidensis MR-1 microbial fuel cells. *RSC Sustainability*. Advance online publication. https://doi.org/10.1039/D5SU00629E

14 Wang, X., Zhang, Y., Zhang, H., & Han, M. (2024). Mechanism analysis of the reduction process of the NiO–YSZ anode of a solid oxide fuel cell by hydrogen. *Journal of The Electrochemical Society, 171*(9), 091501. https://doi.org/10.1149/1945-7111/ad1649.

15 Bekmyrza, K.Zh., Kuterbekov, K.A., Kabyshev, A.M., Kubenova, M.M., Baratova, A.A., Aidarbekov, N., Chaka, M.D., & Benti, N.E. (2025). High-performance hydrogen energy generation via innovative metal-organic framework catalysts and integrated system design. *Scientific Reports, 15*, 28418. https://doi.org/10.1038/s41598-025-08306-6

16 Kuterbekov, K.A., Bekmyrza, K.Zh., Kabyshev, A.M., Kubenova, M.M., Aidarbekov, N.K., & Nurkenov, S.A. (2022). Investigation of the Characteristics of Materials with the Ruddlesden-Popper Structure for Solid Oxide Fuel Cells. *Bulletin of the University of Karaganda — Physics, 108*(4), 32–47. https://doi.org/10.31489/2022ph4/32-47.

17 Nikonov, A.V., Pavzderin, N.B., Khrustov, V.R., Semenova, I.V., Demidova, K.I., Kuterbekov, K.A., Bekmyrza, K.Zh., Nurakov, S.N., Koketay, T.A., & Gyrdasova, O.I. (2021). Investigation of thermal, electrical, and electrochemical properties of $Pr_{1-x}Sr_xFe_{1-y}Co_yO_3$ ($0 < x < 0.4$; $y = 0.2$, 0.5) cathode materials for SOFC. *Journal of Alloys and Compounds, 865*, 158898, https://doi.org/10.1016/j.jallcom.2021.158898.

18 Rakhadilov, B.K., Berdimuratov, N.E., Zhurerova, L.G., Bayatanova, L.B., Kurbanbekov, Sh.R., & Satbayeva, Z.A. (2023). Study of the VAC of the EPCTT process with varying electrode parameters. *Bulletin of the University of Karaganda — Physics, 111*(3), 13632–142.https://doi.org/10.31489/2023ph3/136-142.

19 Li, X., Li, Y., Ren, L., Zhu, K., Zhao, Y., & Yuan, X.-Y. (2017). Self-crosslinking coatings of fluorinated polysiloxanes with enhanced icephobicity. *Thin Solid Films, 638*, 383–390. https://doi.org/10.1016/j.tsf.2017.08.034

20 Zhi, J.H., Zhang, L., Yan, Y.Y., & Zhu, J. (2017). Mechanical durability of superhydrophobic surfaces: The role of surface modification technologies. *Applied Surface Science, 389*, 7–24. https://doi.org/10.1016/j.apsusc.2016.09.049

Г.А. Бакалбаева, А.А. Баратова, Н.К. Айдарбеков,
М.М. Кубенова, А.Н. Амангожаева, Р.С. Бисекен

$Pr_{1-x}Sr_xFe_{1-\gamma}Co_\gamma O_{3-\delta}$ негізіндегі перовскит катодтарының функционалдық қасиеттерін реверсивті қатты оксидті отын элементтері үшін зерттеу

$Pr_{1-x}Sr_xFe_{1-\gamma}Co_\gamma O_{3-\delta}$ құрамындағы перовскиттік катодты материалдардың функционалдық қасиеттері өздігінен таралатын жоғары температуралық синтез әдісі арқылы зерттелді. Зерттеудің негізгі мақсаты — реверсивті қатты оксидті отын элементтерінде (RSOFCs) олардың жұмыс тиімділігін арттыру. Sr және Co изоморфтық орын басуының жылулық ұлғаю коэффициентіне, электрөткізгіштікке және поляризациялық кедергіге әсері қарастырылды. Дилатометриялық талдау, төрт-зондты өлшеу әдісі және электрхимиялық импеданс спектроскопия нәтижелері Sr-дың орташа мөлшері ($x = 0.2$–0.3) ең тиімді теңгерімді қамтамасыз ететінін көрсетті: құрылымдық тұрақтылық сақталады, оттектік вакансиялардың концентрациясы артады және тор параметрлері оңтайланады. Бұл факторлар жоғары электрөткізгіштікке және төмен поляризациялық кедергіге қол жеткізуге мүмкіндік береді. Кобальт қосудың электрондық тасымалдауды күшейтетіні анықталды, алайда оның шамадан тыс мөлшері ($y = 0.5$) жылулық ұлғаю коэффициентін жоғарылатып, электролитпен әрекеттесудің нәтижесінде интерфазалық кедергіні арттырады. Зерттелген үлгілер ішінде PSFC-2020, PSFC-3020 және PSFC-4020 ең жоғары электрхимиялық сипаттамаларды көрсетті: электрөткізгіштік шамамен ~186 $S \cdot см^{-1}$ және поляризациялық кедергі 1.9 $Ом \cdot см^2$-қа дейін төмен 850 °C температурада. Бұл нәтижелер Pr–Sr–Fe–Co негізіндегі перовскиттердің жоғары термомеханикалық үйлесімділігімен, тиімді заряд тасымалдауымен және ұзақ мерзімді тұрақтылығымен RSOFCs катодтары ретінде перспективалы екенін дәлелдейді.

Кілт сөздер: реверсивті қатты оксидті отын элементтері (RSOFCs), перовскит катодтары, Pr–Sr–Fe–Co оксидтері, жылулық ұлғаю, электрөткізгіштік, поляризациялық кедергі, электрхимиялық өнімділік

Г.А. Бакалбаева, А.А. Баратова, Н. К. Айдарбеков,
М.М. Кубенова, А.Н. Амангожаева, Р.С. Бисекен

Исследование функциональных свойств перовскитных катодов $Pr_{1-x}Sr_xFe_{1-\gamma}Co_\gamma O_{3-\delta}$ для реверсивных твёрдооксидных топливных элементов

Проведено комплексное исследование перовскитных катодных материалов состава $Pr_{1-x}Sr_xFe_{1-\gamma}Co_\gamma O_{3-\delta}$, синтезированных методом самораспространяющегося высокотемпературного синтеза, с целью оптимизации их эксплуатационных характеристик в реверсивных твёрдооксидных топливных элементах (RSOFCs). Особое внимание уделялось влиянию замещения Pr стронцием и кобальтом на коэффициент теплового расширения, электропроводность и поляризационное сопротивление в условиях работы элемента. Дилатометрические исследования, измерения проводимости четырёхзондовым методом и электрохимическая импедансная спектроскопия показали, что умеренное содержание Sr ($x = 0.2–0.3$) обеспечивает оптимальное сочетание структурной стабильности, высокой концентрации кислородных вакансий и благоприятных параметров решётки. Эти факторы способствуют росту электропроводности при сохранении низкого поляризационного сопротивления. Введение кобальта усиливает электронный транспорт, однако его избыточное количество (например, $y = 0.5$) вызывает рост коэффициента теплового расширения и увеличение межфазного сопротивления вследствие взаимодействия с электролитом. Наилучшие электрохимические характеристики продемонстрировали составы PSFC-2020, PSFC-3020 и PSFC-4020, обеспечившие проводимость до ~186 $S \cdot см^{-1}$ и поляризационное сопротивление не более 1.9 $Ом \cdot см^2$ при 850 С. Полученные результаты подтверждают перспективность перовскитов Pr–Sr–Fe–Co в качестве эффективных катодов для RSOFCs благодаря их высокой термомеханической совместимости, улучшенной проводимости и долговечности.

Ключевые слова: реверсивные твёрдооксидные топливные элементы (RSOFCs), перовскитные катоды, оксиды Pr–Sr–Fe–Co, тепловое расширение, электропроводность, поляризационное сопротивление, электрохимическая эффективность

Information about the authors

Bakalbayeva, Gulshat — Researcher of the scientific and technical program of the Caspian University of Technology and Engineering named after Sh. Yessenov, Aktau, Kazakhstan; PhD student, L.N. Gumilyov Eurasian National University, Astana, Kazakhstan; e-mail: bakalbayaeva_ga@enu.kz

Baratova, Aliya (*corresponding author*) — Leading researcher of the scientific and technical program of the Caspian university of Technology and Engineering named after Sh. Yessenov, Aktau, Kazakhstan; Candidate of Physical and Mathematical Sciences, Associate Professor, L.N. Gumilyov Eurasian National University, Astana, Kazakhstan; SCOPUS Author ID 55221822500; ORCID ID: 0000-0002-7015-3657; e-mail: baratova_aa@enu.kz

Aidarbekov, Nursultan — Leading researcher of the scientific and technical program of the Caspian university of Technology and Engineering named after Sh. Yessenov, Aktau, Kazakhstan; PhD, Senior Teacher, L.N. Gumilyov Eurasian National University, Astana, Kazakhstan; SCOPUS Author ID: 57222254501; ORCID ID 0000-0002-1981-5416; e-mail: nursultan02_22.10.92@mail.ru

Kubenova, Marzhan — Leading researcher of the scientific and technical program of the Caspian university of Technology and Engineering named after Sh. Yessenov, Aktau, Kazakhstan; PhD, teacher-researcher, L.N. Gumilyov Eurasian National University, Astana, Kazakhstan; SCOPUS Author ID 57197744698; ORCID ID: 0000-0002-7015-3657; e-mail: kubenova_mm_1@enu.kz

Amangozhayeva Arailym — Master student, L.N. Gumilyov Eurasian National University, Astana, Kazakhstan; e-mail: Arai.86-33@mail.ru

Bisseken, Rizabek — Student of 4th course, L.N. Gumilyov Eurasian National University, Astana, Kazakhstan; e-mail: rizabekbisekenov@gmail.ru